Polymer-Regulated Pattern Formation in Pseudo-2D Arrays of a Fullerene Derivative at the Solution–Air Interface

Shani Eliyahu,[1] Chunlai Ren,[2] Igal Szleifer,[3] Rachel Yerushalmi-Rozen[1,4]

[1]Department of Chemical Engineering, Ben-Gurion University of the Negev, 84105 Beer-Sheva, Israel

[2]National Laboratory of Solid State Microstructures, Nanjing University, Nanjing 210093, China

[3]Department of Biomedical Engineering and Chemistry of Life Processes Institute, Northwestern University, 2145 Sheridan Rd., Evanston, Illinois 60208

[4]The Ilze Katz Institute for Nanoscale Science & Technology, Ben-Gurion University of the Negev, 84105 Beer-Sheva, Israel

Correspondence to: R. Yerushalmi-Rozen (E-mail: rachely@bgu.ac.il)

Received 29 October 2010; revised 7 December 2010; accepted 13 December 2010;
DOI: 10.1002/polb.22200

ABSTRACT: Self-assembly of nanoparticles (NPs) into nonclose-packed (ncp), semi-two-dimensional (2D) arrays is of interest in a variety of applications. Of special interest are photochemically active surfactant-like fullerene derivatives [6,6]-phenyl-C_{61}-butyric acid methyl ester (PCBM). The study presented here characterizes the morphology and structure of patterns formed by a mixture of PCBM NP and an amphiphilic block-copolymer tethered at the water–air interface (a surface brush) as a function of the concentration of poly(ethylene oxide) (PEO) dissolved in the liquid subphase. Theoretical modeling of the system shows that the concentration of PEO in the subphase mediates the dimensions of the surface brush and at high PEO concentrations induces a collapse of the brush at the solution–air interface. The state of the surface brush is suggested to tune the semi-2D patterns observed in the experiments via lateral depletion interactions and, in particular, induce lateral phase separation of the PCBM-block copolymer. © 2011 Wiley Periodicals, Inc. J Polym Sci Part B: Polym Phys 000: 000–000, 2011

KEYWORDS: depletion; fullerenes; molecular conformation; nanoparticles; poly(ethylene oxide); polymer brush; polymer layers; self-assembly; surface activity

INTRODUCTION Ordering and self-assembly of nanoparticles (NPs) into mesoscopically large two-dimensional arrays (2D) is a relevant issue in many technological applications. In these systems, the morphology of the assembled suprastructures determines their collective properties. An important group of photochemically active NP are carbonaceous fullerenes and fullerene derivatives[1] such as [6,6]-phenyl-C_{61}-butyric acid methyl ester (PCBM). These serve as the electron accepting moieties when mixed with conjugated polymers in organic photovoltaics.[2] Because of their small diameter (~1 nm) their monodispersity and hydrophobicity PCBM tend to assemble into closely packed aggregates.[3,4] Yet, in many cases nonclose-packed (ncp) 2D patterns are preferred, as they allow for maximization of the NP-matrix interfacial area and the formation of thin layers with tunable electrical and optical properties. The formation of thermodynamically stable or nonequilibrium long-lived structures of ncp 2D patterns requires manipulation of the interparticle interactions.[5] Recently,[6] we reported that a two-component system comprising of PCBM and a nonadsorbing tri-block amphiphilic polymer exhibited a wealth of ncp surface structures at the water–air interface due to in-plain depletion interactions. Randomly oriented micrometric long filaments, coaligned stripes, and networks were observed over macroscopic areas and could be transferred from the water–air interface onto a solid substrate with a high degree of fidelity. Yet the combined system comprising an amphiphilic block copolymer and NP residing at the liquid–air interface are not strictly 2D systems and their phase behavior may be affected by their interactions with the subphase. As was shown theoretically by Zhang et. al.[7] the liquid subphase may be used to tune the formation of NP clusters of different shapes and topology.

Here we present an experimental investigation of the effect of a polymer, poly (ethylene oxide) PEO, dissolved in the liquid subphase on the in-plain phase-behavior and meso-structures formed by a mixture of surfactant-like NP (PCBM), [Fig. 1(a,b)] and a block copolymer (which does not adsorb onto the PCBM) tethered at the solution–air interface to form a polymer brush.[8,9] We find that the concentration of the PEO in the subphase determines the morphology of the mesoscopic semi-2D arrays formed at the interface and the

Additional Supporting Information may be found in the online version of this article.

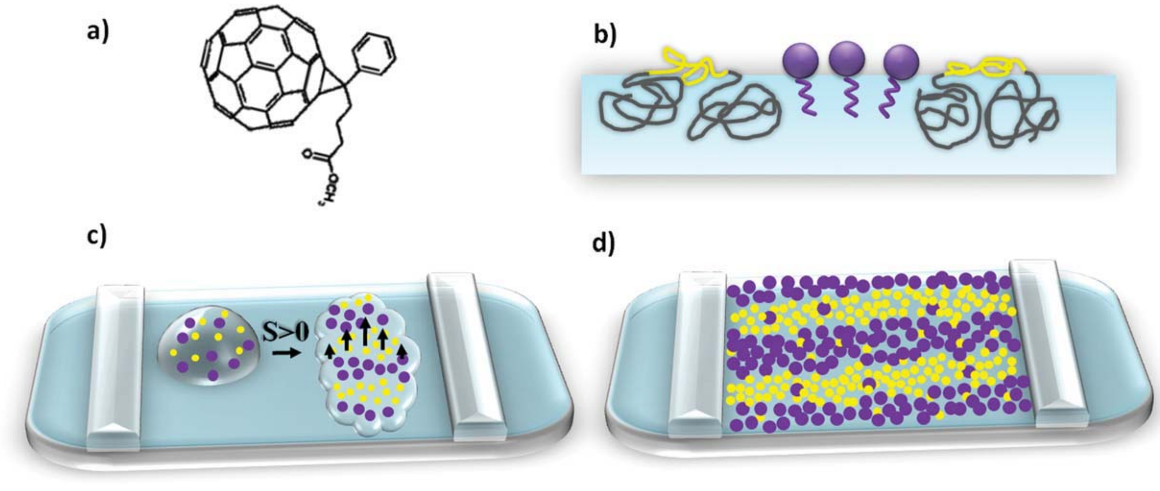

FIGURE 1 (a) Molecular structure of PCBM. (b) Schematics presenting the configuration of PCBM NP[11] and the block-copolymer at the aqueous solution–air interface. (c) The cosolvated PCBM (purple) block-copolymers (yellow) spread at the water–air interface, whereas the carrier solvent, toluene, evaporates. The positive spreading coefficient ($S > 0$)[12] ensures spreading at the solution–air interface. (d) Steady-state patterns at the solution–air interface. [Color figure can be viewed in the online issue, which is available at wileyonlinelibrary.com.]

phase behavior of the NP-block-copolymer mixture. Theoretical modeling of the polymer layer tethered to the liquid–air interface shows that aqueous subphases comprising high concentrations of PEO (above the overlap concentration C^*)[10] lead to a collapse of the surface brush. Consequentially the lateral repulsions between the polymer chains increase. In the block-copolymer PCBM NP mixtures where lateral depletion interactions are active[6,7] the latter results in modification of the surface patterns and at high PEO concentrations in the subphase leads to macroscopic phase separation. The observations described here suggest a pathway for design and preparation 2D arrays of functional NP of different morphologies.

EXPERIMENTAL

Materials

Deionized water (resistivity of 18.3 mΩ), toluene (Gadot, Israel 99.8%), PCBM (99%, Solenne BV, the Netherlands), poly(ethylene glycol) PEO-10K $M_n = 10{,}000$ (Aldrich), F127 ($PEO_{100}PPO_{65}PEO_{100}$, BASF, $M_n = 12{,}600$ g/mol) and 25R4 ($PPO_{32}PEO_{36}PPO_{32}$ $M_n = 4160$ g/mol) (BASF), poly(styrene-*b*-ethylene oxide) ($PS_{35}PEO_{1520}$, $M_n = 70{,}600$ g/mol Polymer source) were used as received.

Sample Preparation

Spreading was carried out from toluene solutions of PCBM and the relevant block-copolymers (F127, 25R4, PEO-PS). The typical dimensions of the polymers in toluene are F127 R_g (toluene) ~5 nm, 25R4 R_g (toluene) ~0.5 nm. Solutions were prepared using deionized water and PEO-10K (R_g (water) ~4.5 nm)[10] at concentrations of 1 wt %, 4 wt % (below and at the overlap concentration, C^* of PEO-10K in water, 3.8 wt %) and 8 wt% were used as the subphase.

The formed patterns were transferred onto solid substrates using the Langmuir–Schaefer method (horizontal lift). Freshly cleaved mica (grade V-5, SPI Supplies, PA), glass (cover slip, Mensel-Glaser, Germany), or perforated polymer film supported on a 300-mesh carbon-coated EM grid (copper, Ted Pella, CA—lacey substrate) were used as substrates. Samples for scanning electron microscopy (SEM) were gold coated. For negative staining one drop of 1 wt % uranyl acetate was applied to a dried sample lifted onto a TEM grid. The drop was blotted after 1 min. The sample was viewed under the electron beam after it was fully dried.

Experimental Procedure

A computerized Langmuir trough (model 622/D1, Nima Technology, Coventry, UK) at effective area between 545–100 cm^2 was used. The spreading solution was placed dropwise on the subphase. The carrier solvent was allowed to evaporate completely (~10 min) before *in situ* characterization was carried out using Brewster angle microscopy (BAM; NFT, Gottingen, Germany). A frequency-doubled Nd:YAG laser with a wavelength of 532 nm and 50 mW primary output power in a collimated beam was used for imaging, and the resulting images were recorded via a CCD camera. A scanner objective (Nikon) of a nominal 10× magnification and diffraction-limited lateral resolution of 2 μm was used. All measurements were carried out at 21 °C.

Characterization Techniques

Surface tension of the solutions was measured using De-Nouy ring tensiometer (model sigma 701, KSV Instruments) at lifting speed of 1 mm/min, and an ambient temperature of 21 °C.

High-resolution transmission electron microscopy (HRTEM, FEI Tecnai 12 G^2 TWIN TEM) and SEM (JEOL JSM-7400F) were used for characterization of the microstructure of the arrays.

Optical phase interference microscopy (OPIM, New View 200, Zygo) was used for profiling patterns of NP transferred onto glass and mica. The setup used in this study offers

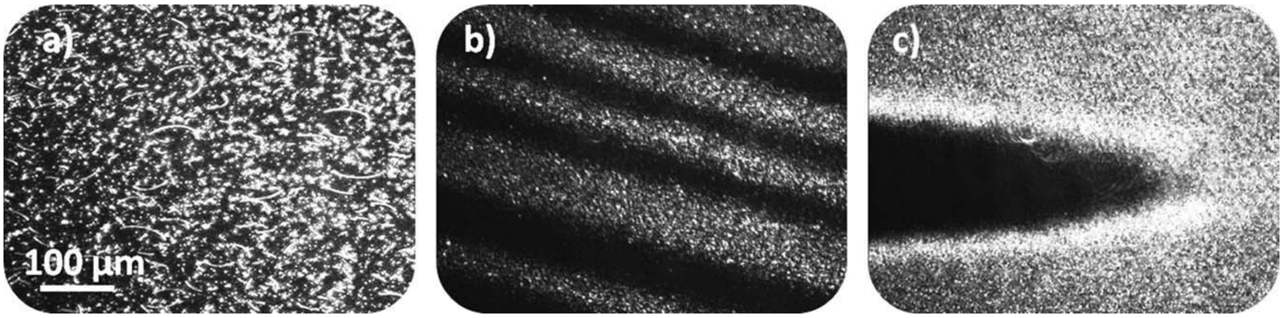

FIGURE 2 *In situ* BAM images of PCBM assemblies formed following the spreading of a PCBM–F127–toluene solution and complete evaporation of the solvent. The molar ratio of PCBM to F127 is 1:0.48 at a calculated (initial) surface area per PCBM NP of 2.75 nm^2. (a) Water subphase, b) subphase of 1 wt % PEO solution $C_{\mathrm{subphase}} < C^*$, (c) subphase of 4 wt % PEO solution $C_{\mathrm{subphase}} \sim C^*$. Regions of high NP concentration appear bright, whereas polymer rich regions are dark.

subnanometric resolution in the vertical direction, a lateral resolution of 0.64 μm, and a maximal field of view of 280 × 220 μm^2. In this technique, a beam of white light that scans the sample is reflected from the surface and interferes with a reference beam, to generate an interference pattern that is monitored by a CCD camera. The pattern is analyzed using a computerized algorithm (frequency domain analysis) to obtain a quantitative 3D image of the sample.

RESULTS

A schematic illustration of the components [Fig. 1(a,b)] and the experiment [Fig. 1(c,d)] is presented. In a typical experiment, droplets of a toluene solution of the NP-block-copolymer mixture are placed at the water–air or solution–air interface using a syringe. The droplets of the organic solution readily spread on the subphase [6] [Fig. 1(c)] while the immiscible solvent evaporates. Following solvent evaporation (10 min) and reorganization of the components the patterns formed at the liquid–air interface [Fig. 1(d)] are recorded *in situ* using BAM (Fig. 2).

Figure 2 presents *in situ* BAM images formed spontaneously at the liquid–air interface by a mixture of PCBM NP and $\mathrm{PEO_{100}\ PPO_{65}\ PEO_{100}}$, F127 (molar ratio PCBM:F127 of 1:0.48). The bright areas in the pictures are PCBM-rich areas, and the polymer is invisible to the BAM.

On a water subphase [Fig. 2(a)], randomly oriented filaments are observed, whereas a stripe pattern is observed to form on an aqueous solution of 1 wt % PEO-10K [Fig. 2(b)][6], and macroscopic phase separation takes place when the subphase is a PEO-10K solution of 4 wt % [Fig. 2(c)].

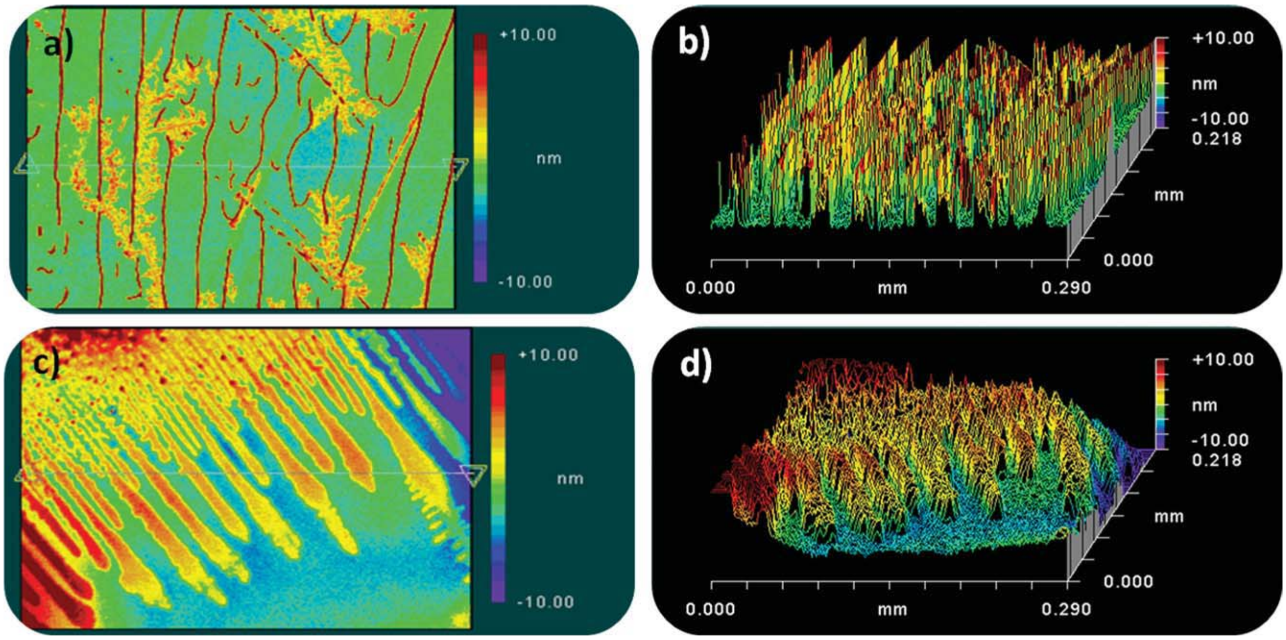

FIGURE 3 OPIM images of PCBM–F127 (molar ratio PCBM:F127 of 1:0.48) patterns transferred onto a mica substrate from (a,b) water interface (c,d) aqueous solution of PEO (1 wt %). Note that OPIM, which is an interference scanning microscopy technique, provides nanometric height resolution and lateral resolution of microns (see the experimental part). [Color figure can be viewed in the online issue, which is available at wileyonlinelibrary.com.]

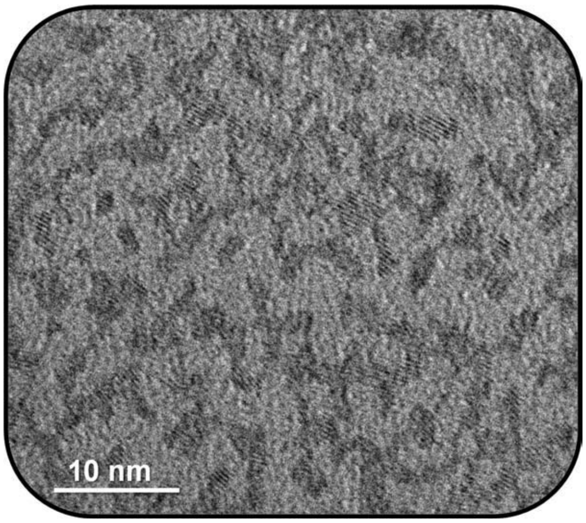

FIGURE 4 TEM image of a specimen taken from the water–air interface in a region exhibiting the structure presented in Figure 1(a) (PCBM: F127 molar ratio of 1:0.48). The sample was dried and negatively stained with uranyl acetate following the procedure described in the text. The typical spacing among the dark stripes is 0.34 nm.

The filaments and stripes were transferred onto solid substrates and investigated *ex situ* using interference microscopy (OPIM; Fig. 3) and HRTEM (Fig. 4). The typical height of the filaments was found to be about 20 nm [Fig. 3(a,b)] while their width and length are few microns and some hundred microns, correspondingly. The stripes are typically thinner and broader [Fig. 3(c,d)] with a thickness of about 7 nm, length of several hundreds of microns and width of tens of microns.

In Figure 4, we present HRTEM images of a filament forming sample [as in Fig. 2(a)].

The HRTEM images of a uranyl-stained sample transferred from the water surface reveal the nanometric structure of the patterns. The observed contrast probably results from preferential adsorption of the positive uranyl ions to the PCBM clusters (dark regions).[13] The patchy structure observed in Figure 4 is consistent with the UV–vis measurements of a similar system presented by us in a previous publication,[6] where it was found that in a PCBM–F127 mixture, the samples exhibit solution-like spectra and lack the spectroscopic features that characterize single-component close-packed PCBM films. The results indicate that the two components are comixed within the filaments.

To test the role of the surface tri-block-copolymer in the observed behavior we replaced the F127 polymer by a short, relatively hydrophobic block copolymer, $PPO_{32}PEO_{36}PPO_{32}$, 25R4.

In Figure 5, we present *in situ* BAM images of PCBM arrays and clusters formed spontaneously by a mixture of PCBM and 25R4. Examining the behavior of the mixture on a water subphase, we find that at a similar molar ratio to that presented in Figure 2(a) a collection of unconnected islands forms. At a PCBM:25R4 molar ratio of 1:1.68 a network structure emerges. These networks patterns were discussed by us previously.[6] Here, we find that unlike the patterns presented in Figure 2, the networks are not sensitive to the presence of PEO in the subphase [Fig. 5(b,c) and Supporting Information Fig. S1]. The microstructure of the cell walls of the networks was investigated using HRSEM (Fig. 6) showing a fractal-like pattern.

In an additional set of experiments PCBM was codissolved with a diblock copolymer $PS_{35}PEO_{1520}$. The polymer is known to adsorb onto the PCBM NPs forming micelles, which incorporate the PCBM into the hydrophobic core.[14] The solution was spread on water following the experimental procedure described above. The BAM images presented in Figure 7(a) indicate that a close-packed array of polymer-coated NPs assembles at the water–air interface, very differently from the structures formed in the presence of the non-adsorbing polymers.

A control experiment was performed where PCBM was dissolved in toluene and spread on top of the subphase. We found that in the absence of a codissolved, nonadsorbing block copolymer PCBM aggregated into closely packed arrays. The aggregation was found to be irreversible and the features of the densely packed film were similar to those reported in previous studies of similar fullerene derivatives at the water–air interface[11] suggesting that the NP are

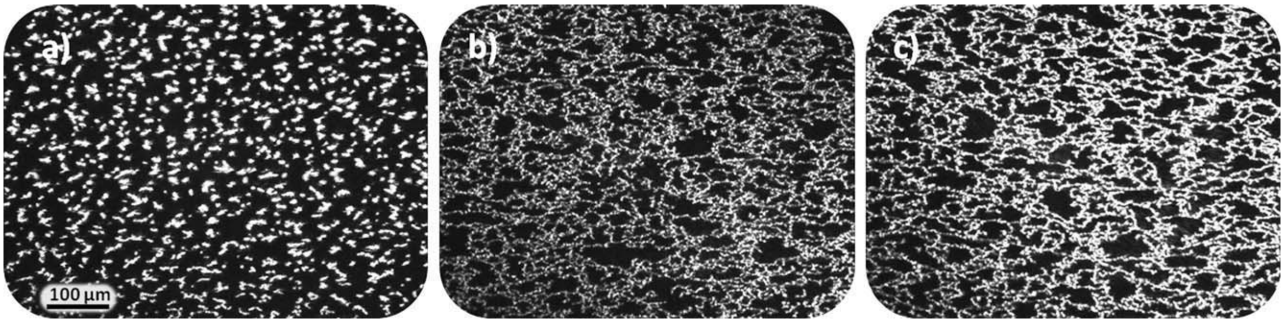

FIGURE 5 *In situ* BAM images of PCBM assemblies formed following the spreading of a PCBM–25R4–toluene solution at the air-aqueous solution interface at 2.75 nm^2 per NP. (a) PCBM-25R4 at a ratio of 1:0.5 spread on water interface. (b) PCBM: 25R4 at a molar ratio of 1:1.68 on water (c) same as (b) but on 1 wt % PEO-10K solution.

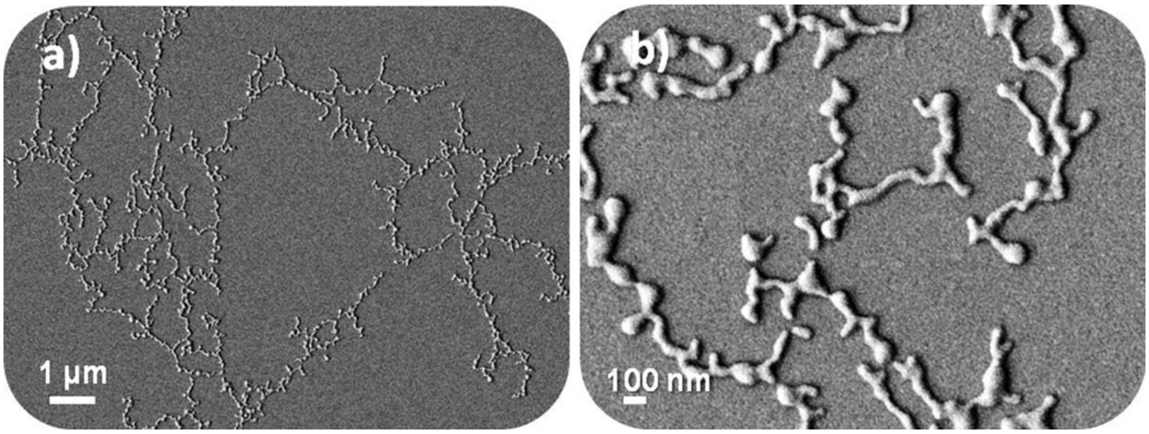

FIGURE 6 SEM images of network structure formed on a water subphase from a toluene solution of PCBM-25R4 at a molar ratio of 1:1.68. The samples were collected on glass following the procedure described in the text and gold coated.

closely packed with the hydrophilic moiety oriented toward the water phase [as schematically presented in Fig. 1(b)]. In Figure 7(b), we present a BAM image of the arrays formed on a water subphase and in the Supporting Information (Fig. S2) similar arrays formed on a PEO-10K subphase (1 and 4 wt %). HRTEM (Supporting Information Fig. S3) substantiates the close-packed structure of the pseudo-2D arrays.

DISCUSSION

In this study, we investigated the effect of a polymer dissolved in the liquid subphase on the self-assembly and pattern formation in a system comprising of codissolved PCBM NP and a triblock copolymer that does not adsorb onto the NP and forms a brush layer at the water–air interface. We found that spreading of the NP-block copolymer mixture from a common (good) solvent at the interface between an aqueous solution of PEO and air resulted in the formation of a variety of patterns. The spreading was followed by partial evaporation of the solvent and consequential rearrangement of the NP and the block-copolymer at the air–water interface. As was discussed by us previously,[6] in this system, solvent evaporation effectively increases the concentration of the components and leads to the onset of aggregation due to lateral depletion interactions among the NP and the codissolved block-copolymer molecules. The resulting patterns are shaped by the sequence and details of the evaporation mechanism.[15,16] As solvent evaporation is not instantaneous on the time scale of the particles and polymers dynamics, in-plane diffusion may lead to the formation of macroscopic domains such as filaments and stripes under the combined action of lateral and interfacial interactions as well as interactions with the liquid subphase. The observed patterns may be intermediate states quenched by solvent evaporation before macroscopic phase separation has been achieved.

In this study, we find that PEO homopolymer dissolved in the subphase significantly affects the morphology and phase behavior of the system: In particular, we observe that in a mixture of F127 ($PEO_{100}PPO_{65}PEO_{100}$) and PCBM

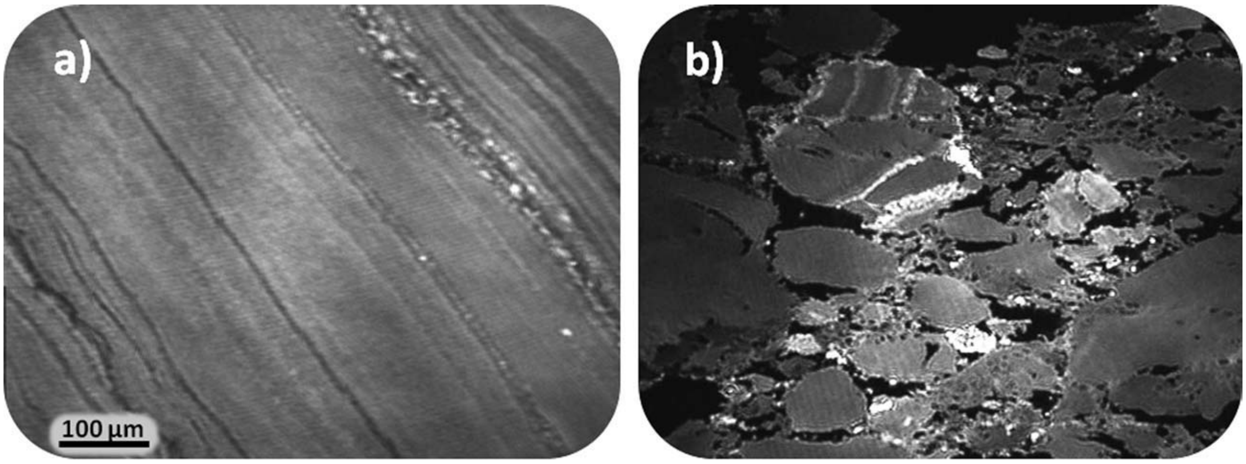

FIGURE 7 *In situ* BAM images of close packed arrays resulting from spreading toluene solutions of (a) PCBM and PS-PEO block-copolymer on water interface (at PCBM: polymer molar ratio of 1:0.085). (b) PCBM (from organic solution with a concentration of 1.5 mg/mL) on water interface.

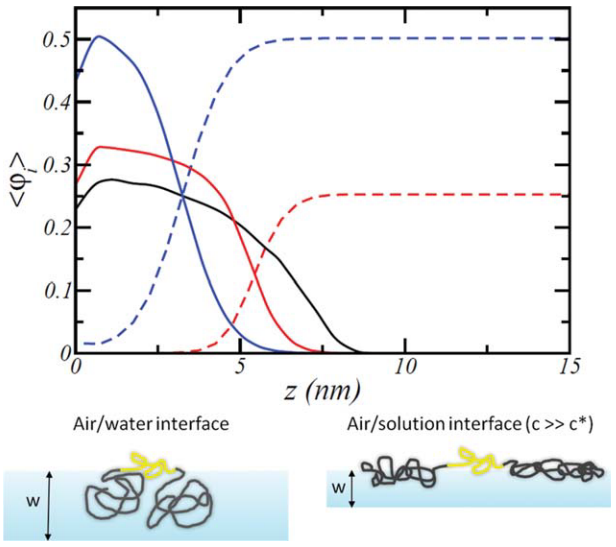

FIGURE 8 The volume fraction of the grafted polymers (full lines) and bulk PEO (dashed lines) as a function of the distance from the surface. All the cases correspond to the same surface density of polymer, $\sigma = 0.1$ nm^{-2}, while the different colors correspond to different bulk concentrations of PEO: black $\phi_{\text{bulk}} = 0$; red $\phi_{\text{bulk}} = 0.25$ and blue $\phi_{\text{bulk}} = 0.5$. The semidilute regime for of the bulk polymer is calculated from the theory to be $\phi^* = 0.1$. The grafted polymer has a chain length of $n = 50$, while the bulk polymer corresponds to $n = 100$, keeping the same ratio of chain lengths as in the experimental studies. The bottom cartoons denote a schematic showing the collapse of the tethered polymer at the air–solution interface, representing the theoretical calculations.

nonisotropic high aspect ratio PCBM clusters form on a water subphase, whereas macroscopic phase separation takes place when the subphase is a PEO solution at the overlap concentration, *C** of the polymer. We suggest that the key feature that determines the interfacial behavior of the combined system is the interactions of the block-copolymer grafted at the water–solution interface. These interactions, however, are tuned by the PEO in the subphase. We find through theoretical calculations, see Supporting Information and ref. 17 that increasing the bulk concentration of PEO results in a sharp collapse of the grafted chains. This collapse is not due to a change in the quality of the solvent[18] as it happens in low-molecular weight solvents. Rather, the collapse of the chains is due to an entropic repulsion, in which the collapse of the brush chains allows for a maximal entropic gain of the polymers in the solution, see Figure 8. In other words, the quality of the solvent is changed from good to poor by an entropic rather than energetic driving force, with the net result that the presence of the polymers in solution effectively collapses the brush. It is important to stress that this is not a brush to mushroom transition because it happens at fixed surface coverage of the grafted chains.

As a direct consequence, the collapsed F127 molecules occupy a larger effective area per chain at the interfacial plane.[19,20] Consequentially, the collapsed chains experience enhanced in-plane repulsive (steric) interactions in the F127–PCBM mixtures leading to macroscpic phase separation into PCBM-rich and F127-rich domains [Fig. 2(d)]. This scenario is supported by the observation of the second system studied here where F127 is replaced by a short, relatively hydrophobic block-copolymer ($PPO_{32}PEO_{36}PPO_{32}$, 25R4) where the surface patterns are not affected by the concentration of PEO in the subphase (Fig. 5). Indeed, for the short chains, the collapse of the grafted "brush" due to a high concentration of PEO in the solution does not result in a dramatic change in the lateral repulsions. In this system, networks of polygonal cells (Voronoi cell structures[21]) are consistently observed.

In this study, we also found that the presence of a nonadsorbing polymer is necessary for the formation of nonclose-packed patterns of pseudo-2D arrays of PCBM–NP: both native solutions of PCBM (in toluene) and solutions containing an adsorbing polymer, PS–PEO were observed to induce the formation of close-packed arrays at the interface, irrespective of the subphase. In these systems, the attractive interparticle interactions seem to dominate over the interactions with the subphase.

The study presented here demonstrates that a combined system comprising a tethered surface brush and a homopolymer dissolved in the liquid subphase may be used for engineering the morphology of ncp patterns of NP. Essentially, a nonadsorbing block-copolymer interacts via (entropic) depletion interactions with the NP thus offering a generic mechanism that is applicable to a variety of NP (gold NP, semiconducting NP) and different, commercially available block copolymers. Moreover, the use of a nonadsorbing polymer as a structure-mediating agent is advantageous for applications that rely on the electronic and optical properties of the pristine-unmodified NP.

ACKNOWLEDGEMENTS

The support of the BSF—United States-Israel Binational Science Foundation and the Israel Science Foundation is acknowledged. R.Y.-R. holds the Stanley D. and Nikki Waxberg professorial chair in Advanced Materials. IS also acknowledges the National Science Foundation for partial support of this work under grant CBET-0828046.

REFERENCES AND NOTES

1 Wang, X. K.; Zhang, T. G.; Lin, W. P.; Sheng, Z. L.; Wong, G. K.; Kappes, M. M.; Chang, R. P. H.; Ketterson, J. B. *Appl. Phys. Lett.* **1992,** *60*, 810–812.

2 Blom, P. W. M.; Mihailetchi, V. D.; Koster, L. J. A.; Markov, D. E. *Adv. Mater.* **2007,** *19*, 1551–1566.

3 Oosterhout, S. D.; Wienk, M. M.; van Bavel, S. S.; Thiedmann, R.; Koster, L. J. A.; Gilot, J.; Loos, J.; Schmidt, V.; Janssen, R. A. *J. Nat. Mater.* **2009,** *8*, 818–824.

4 Mendoza, D.; Gonzalez, G.; Escudero, R. *Adv. Mater.* **1999,** *11*, 31–33.

5 Cheyne, R. B.; Moffitt, M. G. *Langmuir* **2005,** *21*, 10297–10300.

6 Eliyahu, S.; Yerushalmi-Rozen, R. *Chem. Commun.* **2010,** *46*, 5966–5968.

7 Zhang, D.; Carignano, M. A.; Szleifer, I. *Phys. Rev. Lett.* **2006,** *96*, 028701-1–028701-4.

8 Halperin, A.; Tirrell, M.; Lodge, T. P. *Adv. Polym. Sci.* **1992,** *100*, 31–71.

9 Hussain, H.; Kerth, A.; Blume, A.; Kressler, J. J. *Phys. Chem. B* **2004,** *108*, 9962–9969.

10 A measure of the diameter of the volume occupied by a polymer chain in a good solvent is the gyration radius R_g (nm) $= a\ (C_\infty N/6)^{1/2}$. For PEO $a = 0.28$ nm, $C_\infty = 4.25$ and N is the number of repeat units of the polymer chain. The overlap concentration, at which dissolved polymer chains begin to overlap, and become semi-dilute, can be calculated from the relation $C^* = 3M_w/4\pi R_g N$.

11 Matsumoto, M.; Tachibana, H.; Azumi, R.; Tanaka, M.; Nakamura, T.; Yunome, G.; Yamago, M. A. S.; Nakamura, E. *Langmuir* **1995,** *11*, 660–665.

12 Spreading occurs due to the positive value of the spreading coefficient $S = \gamma_{aqu/air}\text{-}\gamma_{tol/air}\text{-}\gamma_{tol/aqu}$ ~8 mN/m, where $\gamma_{aqu/air}$ is the interfacial tension at the aqueous subphase-air interface, $\gamma_{tol/air}$ is the interfacial tension of the relevant spreading solution and $\gamma_{aqu/tol}$ is the interfacial tension at the relevant aqueous subphase and the spreading solution interface. The calculated spreading coefficient is positive and as the toluene evaporates the tendency towards spreading increases (for details see ref. 5).

13 Chase, S. J.; Bacsa, W. S.; Mitch, M. G.; Pilione, L. J.; Lannin, J. S. *Phys. Rev. B* **1992,** *46*, 7873–7877.

14 Schmaltz, B.; Brinkmann, M.; Mathis, C. *Macromolecules* **2004,** *37*, 9056–9063.

15 Rabani, E.; Reichman, D. R.; Geissler, P. L.; Brus, L. E. *Nature* **2003,** *426*, 271–274.

16 Kletenik-Edelman, O.; Sztrum-Vartash, C. G.; Rabani, E. *J. Mater. Chem.* **2009,** *19*, 2872–2876.

17 Szleifer, I.; Carignano, M. A. *Adv. Chem. Phys.* **1996,** *94*, 165–260.

18 Jones, R. A. L.; Richards, R. W. Polymers at Surfaces and Interfaces; Cambridge University Press: Cambridge, **1999;** pp 317–371.

19 Cao, B. H.; Kim, M. W. *Faraday Discuss* **1994,** *98*, 245–252.

20 Kim, M. W.; Cao, B. H. *Europhys. Lett.* **1993,** *24*, 229–234.

21 Getis, A.; Boots, B. Models of Spatial Processes; Cambridge University Press: Cambridge, **1978;** pp 87–90.